

# Wind Wave Effect on the Sea Surface Measurements

Yuri Trokhimovski

Space Research Institute (IKI), Russian Academy of Sciences

ytrokh@mx.iki.rssi.ru

L-band brightness temperature of the sea surface as a function of wind speed was studied only in a few experiments. Such measurements are of high importance for appropriate determining the ocean salinity by microwave radiometers. During Russian experiments at aircraft AN-12 (1981-1989) L-band radiometer was mounted at nadir view angle. Fig. 1 shows an example of the sea surface brightness temperature variation caused by variable wind speed at different wavelengths. All measurements were made at nadir view angle. It is seen, that amplitude registered at L-band is a few times smaller, than amplitude at K- and K-u band. Using similar data it was determined "wind speed sensitivity"  $\frac{\partial T_{Br}}{\partial V}$  at moderate wind conditions. Results are given in Fig. 2. The data used for analysis include measurements at view angles 0, 10 and 20 degrees from the nadir. Wind sensitivity at L-band is of about 0.18 K/(m/s) and is about the same for upwind-downwind and crosswind view. The amplitude of wind sensitivity is in good agreement with results of *Hollinger* [1971] ( $f=1.41$  GHz, Fig. 3) and results reported by *Blume et al.* [1977] ( $f=2.65$  GHz, Fig 4).

*Electromagnetic theory.* The electromagnetic theory to calculate brightness temperature of the water surface covered by wind waves is well developed. The brightness temperature is calculated in frame of the composite model. The contribution of long waves is determined in frame of the Kirchhoff approach. Appropriate accuracy can be realized by averaging the emissivity coefficient (which depends on local incident angle) over slope distribution of long waves. The same procedure is applied to the sky radiation reflected from the water surface. It is possible to shown, that for the majority of angles the contribution of long waves is approximately proportionally to the mean squared slope of these waves:

$$\Delta T_{BL}(k_0) = F(\langle s^2 \rangle) = a\langle s^2 \rangle + o(\langle s^2 \rangle)^2,$$

where  $\langle s^2 \rangle$  is the mean square slope of sea surface.

The same approach is absolutely wrong for short waves. Diffraction is important in this case and one have to use small perturbation technique of the second order (or small slope expansion) to calculate brightness temperature. It is possible to show that if the slope of the surface is small, we can calculate the contribution of different harmonics separately and determine total contrast of short waves by integrating over small-scale wavenumbers:

$$\Delta T_{BL}(k_0, \mathbf{j}_0) = \int_{-p}^p \int_{k_s}^{\infty} B(k, \mathbf{j}) \cdot D(k, \mathbf{j} - \mathbf{j}_0) \cdot k dk d\mathbf{j} ,$$

where  $B(k, \mathbf{j})$  is two-dimensional symmetrical curvature spectrum,  $D$  is a function which determines the contribution of different harmonics to brightness temperature contrast due to surface emission and scattered sky radiation,  $k_0$  is the wavenumber of the electromagnetic radiation,  $\mathbf{j}_0$  is the azimuthal angle of observation, and  $k_s$  is the separation wavenumber between large-scale and small-scale harmonics. Although, we have not shown additional variables in  $D$ , this function in general depends on the electromagnetic wavenumber  $k_0$ , the water dielectric permittivity, polarization, nadir angle, and total atmospheric absorption.

First variant of second order perturbation theory was proposed for one-dimensional case by *Kravtsov, Mirovskaya, Popov, Troickii, Etkin* [1978]. It was found that, there is strong increase of the brightness temperature at the resonant condition  $K = k(1 \pm \sin \theta)$ . Next, theory was extended for two-dimensional case Fig. 5. Small perturbation technique was verified in modeling experiments. Fig. 6 shows results obtained in a tank with waves generated by a mechanical plunger. Next, a technique was proposed to form periodic structure on water surface by a system of parallel nylon strings Fig. 7. Using this technique the effect of short roughness was studied both for small Fig. 8 and large amplitudes Fig. 9. Initially, we have made measurements by an ordinal microwave radiometer for a variety of roughness periods on water surface. Finally, a set of measurements was made using radio-interferometer Fig. 10 for a fixed roughness.

Results based on small perturbation technique were also compared with calculation based on numerical solution of Maxwell equation, valid for arbitrary amplitude of surface roughness Fig. 11. It was noted, that if short wave contribution is small (say less than 20 K) so small perturbation approach provide high accuracy.

Very important, that small perturbation results are in agreement with results based on Kirchgoff method for long waves. As was noted by V. Irisov (and previously by I. Fuks) results based on small perturbation technique are indeed expansion in wave slope and for this reason are valid for long waves of large amplitude provided their slope is small. A comparison between calculation based on Kirchgoff method and small perturbation technique is given in Fig. 12. For long waves, the only difference between two methods is coming from reflected atmospheric radiation, but in general this difference is not too high. Hence, the choice of the separation wavenumber between long and short waves can be made quit arbitrary, the only criteria is that separation wavenumber must be much smaller than electromagnetic wavenumber to account all diffraction phenomenon. Usually, we take the separation wavenumber equal to  $k_s=0.05k_0$  (*Trokhimovski et al.* [2000], *Trokhimovski* [2000]). Expressions for short wave contribution are published recently in English by *Irisov* [2000].

*Wave spectrum.* The form of the ocean surface is still not known very well. It is extremely difficult to measure spectrum of short waves, needed for adequate modeling. Although a series of experiments have been undertaken over the last 20 years to collect suitable measurements by optical and microwave radar technologies, our knowledge in this area is far from satisfactory. The scatter of different models and reported tank and field experimental results are dramatically large and the predicted spectral density can be different by one order or more. Currently, three main approaches are used for gravity-capillary wavenumber spectrum investigations. The first approach is based on field measurements by scanning laser slope sensors (Hara et al. 1994; Hwang et al. 1996; Hara et al. 1998) and the second considers the sea surface radar backscatter with an adjustment of spectral parameters to provide the best fit with radar data (Donelan and Pierson 1987; Apel 1994; Romeiser et al. 1997). The last technique is based on an analysis of polarimetric microwave measurements of the sea surface brightness temperature. A retrieval of the gravity-capillary spectrum is made from the elevation angular dependence of the ocean surface microwave emission at vertical and horizontal polarizations. The idea that the sea surface brightness temperature contrasts could be converted to spectrum parameters was formulated by Prof. V. S. Etkin about 20 years ago. The first estimation was performed from nadir radiometric measurements at wavelengths 0.8, 1.5, 2, and 8 cm under the assumption that spectral density obeys a power law of wavenumber (Irisov et al. 1987a). Further experimental studies by optical techniques and analysis of radar backscatter have shown that the power-law approximation is not appropriate to describe spectral density in the gravity-capillary interval. Trokhimovski (1997) has proposed an approach to retrieve waves parameters from a set of radiometric measurements collected at several angles, polarizations, and wavenumbers without any a priori assumption about the spectrum shape.

Spectrum developed by *Donelan and Pierson* [1987], *Apel* [1994], *Romeiser et al.* [1997], and *Elfouhaily et al.* [1997] are given in Fig. 13. The first three models above use wind speed as a modeling input; the last uses friction velocity. We used wind speed of 7.3 m/s for the first three and a value of 24 cm/s for the last. In the remainder of this presentation, we will label these models as D, A, R, and E. Fig. 13 shows the omnidirectional spectrum  $B(k)$  determined in such a way that:

$$B(k, \mathbf{j}) \cdot k dk d\mathbf{j} = B(k) \cdot W(\mathbf{j}) \cdot k dk d\mathbf{j} , \text{ and}$$

$$\int_{-p}^p W(\mathbf{j}) d\mathbf{j} = 1 ,$$

where  $B(k, \mathbf{j})$  is the two-dimensional symmetrical curvature spectrum,  $B(k)$  is the dimensionless omnidirectional curvature spectrum, and  $W(\mathbf{j})$  is the spreading function. Note that in some papers the spreading function is normalized by its maximum in downwind direction, so we have made a proper correction. It is obvious that spectrum densities are essentially different for different models. The mean squared slope supported by long waves also varies.

The have considered also “*Best fit spectrum*” retrieved by *Trokhimovski* [1997] using microwave radiometric data collected in different experiments. The spectrum shape at wind speed 10 m/s is given in Fig. 14. To recalculate spectrum density to arbitrary wind speed we assume that spectrum density depends on wind speed as  $V^\gamma$  with wind exponent:

$$\gamma = \begin{cases} 0.21 + 0.72k & k < 3 \text{ rad/cm} \\ 2.3 & k \geq 3 \text{ rad/cm} \end{cases}$$

The last approximation was obtained using microwave radiometric and radar data analyzed by *Trokhimovski and Irisov* [2000].

*Modeling.* The microwave brightness temperature contrast of the sea surface, defined as the difference between the brightness temperature observed at some sea state and the brightness temperature of the smooth water surface with the same physical parameters (temperature and salinity), was calculated using various models of wind waves. The brightness temperature of a smooth water surface was found under the assumption that the atmosphere is horizontally uniform and that it is possible to attribute an effective temperature for total column of the atmosphere. Comparison with experimental data collected at wind speed 10 m/s is given in Fig. 15 for view angle 50 degrees from the nadir and in Fig. 16 for nadir view. All data are plotted versus radiometric frequency. It is natural that, the “*Best fit spectrum*” is in a perfect agreement with data, because it was retrieved just from this data set. Spectrums by *Donelan and Pierson* [1987], *Apel* [1994], *Romeiser et al.* [1997] in most cases predict too large values of the brightness temperature contrast, especially in L-band. Brightness temperature contrast in L-band at wind speed 10 m/s is well described by modeling based on *Elfouhaily et al.* [1997] spectrum.

Next, we have tested the “*Best fit spectrum*” and *Elfouhaily et al.* [1997] spectrum in a modeling of the wind sensitivity, defined as  $\partial T_B / \partial V$ . Strong to say, the brightness temperature is not leaner function of the wind speed and value  $\partial T_B / \partial V$  depends on wind speed. But, in C-band the relationship between wind and brightness temperature is very close to the linear low. The same is true in L-band if one excludes from the consideration very low wind velocities (less than 2 m/s). Modeling results at nadir view are given in Fig. 17 where,  $\partial T_B / \partial V$  is plotted versus radiometric frequency. Next figures (Fig. 18, 19) show  $\partial T_B / \partial V$  in C-band versus view angle both for horizontal and vertical polarizations. It is obvious some drawback of the model by *Elfouhaily et al.* [1997]. It seems, that this model predict too week wind speed dependence.

L-band theoretical results obtained using “*Best fit spectrum*” and *Elfouhaily et al.* [1997] spectrum are shown in Fig. 20. The difference is obvious. Our impression is that wind dependence predicted by “*Best fit spectrum*” model is more adequate. In the same time *Elfouhaily et al.* [1997] spectrum demonstrate important feature at low wind speed – some offset of the brightness

temperature contrast, which was really observed in our experiments at very low wind speed. This phenomena is illustrated in Fig. 20.

*Azimuthal dependence.* The azimuthal dependence of the L-band brightness temperature was measured only in a limited number of experiments. More extended study was made in C-band. Fig. 21 shows three example of C-band results from paper by *Trokhimovski and Irisov*. [1995 ]. Note, that amplitude of second harmonic is very small, much smaller than in K-band. Only at very strong wind it is reasonable to account the azimuthal dependence of the C-band brightness temperature. It is reasonable to expect smaller value at L-band, but only a few measurements are available.

### *Conclusions*

1. Electrodynamics theory is well developed.
2. Wind wave spectrum is the most critical point in modeling. Still, we have no adequate spectrum model, which explains all known experimental results.
3. The spectrum model can be improved using precise C- and L-band measurements from aircraft or sea platform. Important is to measure absolute brightness temperature at vertical and horizontal polarization for view angles  $0\div 60^\circ$ , wind speed  $0\div 12$  m/s.
4. Upwind/downwind difference is of 0.2 K in C-band at wind speed 10 m/s. It is reasonable to expect smaller value at L-band, but only a few measurements are available. New measurements are of high importance. It is important also to perform accurate analysis of L-band measurements (nadir) collected in Russian experiments on aircraft AN-12.
5. At high wind speeds the contribution of foam must be included in modeling.
6. For practical application like SMOS data modeling and inverse problem solution it is important to elaborate simple model function  $\Delta T_B = F(V, \theta)$ . This function must be based on a compromise between available experimental data and results of modeling.
7. SMOS instrument provide unique angular measurements of the sea surface brightness temperature. For that reason, new approaches could be applied in inverse algorithms. It might be, that it is not needed to select between different spectrum model to describe wind wave influence, but to determine some spectrum parameters direct from the ocean brightness temperature measurements. Final decision must be made after extended numerical simulation.

### *References*

- Apel J. R., "An improved model of the ocean surface wave vector spectrum and its effects on radar backscatter", vol. 99, no. C8, pp.16269-16291, 1994.
- Blume H.J.C., Love A.W., Van Melle M.J., Ho W.W. Radiometric observation of sea surface temperature at 2.65 GHz over the Chesapeake Bay // IEEE Trans. on Antennas and Propagat. 1977. P. 121-128.
- Donelan M. A., and W. J. Pierson, "Radar scattering and equilibrium ranges in wind-generated waves with application to scatterometry", J. Geophys. Res., vol. 92, pp. 4971-5029, 1987.
- Elfouhaily T., B. Chapron, K. Katsaros, and D. Vandemark, "A unified directional spectrum for long and short wind-driven waves", J. Geophys. Res., vol.102, no. C7, pp.15781-15796, 1997.
- Etkin V.S., Vorsin N.N., Kravtsov Yu.A., Mirovski V.G., Nikitin V.V., Popov A.E., Troitski I.A. Discovering Critical Phenomena under Thermal Microwave Emission of the Uneven Water Surface. Radiophysics and Quantum Electronics, v.21, No.3, 454-456, 1978. (in Russian)
- Etkin V.S., Irisov V.G., Trokhimovski Yu.G. Resonant Radiothermal Emission of Water Surface with Non-Small Periodic Roughness, Proc. Int. Geoscience and Remote Sensing Symp. (IGARSS'92), Houston, USA, 1457-1459, 1992.
- Gershenson V.E., Irisov V.G., Trokhimovski Yu.G., Etkin V.S. Investigation of Resonant Effects in the Radiothermal Emission of Water Surface. Radiophysics, v.29, No.4, 379-384, 1986. (in Russian)
- Gershenson V.E., Irisov V.G., Trokhimovski Yu.G., Etkin V.S. Azimuthal Effects of Critical Phenomena in the Thermal Emission of a Rough Surface. Space Research Institute Tech. Memo., Pr-1104, 23p., 1986. (in Russian)
- Gershenson V.E., Irisov V.G., Trokhimovski Yu.G., Etkin V.S. Critical Phenomena in the Thermal Radiation of Uneven Water Surface at Arbitrary View Angles. Radiophysics, v.30, No.9, 1159-1163, 1987. (in Russian)
- Hollinger J.P. Passive microwave measurements of the sea surface // J. of Geophys.Res. 1970. V. 75. P. 5209-5213.
- Isozaki I., Ueno K., Iida H., Hayashi S., Shibata A., Igarashi T. Observation of sea surface microwave emission (2nd report) // in Proc. Autumnal Meeting Oceanogr. Soc. Japan. 1984. P. 143-144.
- Irisov V.G. Studies of Electromagnetic Waves Radiation of a Periodically Uneven Surface. Space Research Institute Tech. Memo., Pr-944, 18p., 1984. (in Russian)
- Irisov V.G., Trokhimovski Yu.G., Etkin V.S. The Radiometric Methods of the Ocean Diagnostics. In a book: Remote Techniques for Oceanic Research, 34-58, 1987. (in Russian)
- Irisov V.G., Trokhimovski Yu.G., Etkin V.S. Radiothermal spectroscopy of the ocean surface, Sov. Phys. Dokl., v. 32, p. 914-915, 1987.
- Irisov V.G. Small slope approximation for microwave polarimetric observation of sea surface // Proc. IGARSS'94., P. 2421-2423, 1994a.

- Irisov V.G. Small-slope expansion for electromagnetic-wave diffraction on a rough surface // *Waves in random media*, V. 4. P. 441-452, 1994b.
- Irisov V.G. Azimuthal variations of the microwave radiation from a slightly non-Gaussian sea surface. *Radio Science*, V. 35., No 1, p. 65-82, 2000.
- Il'in V.A., Irisov V.G., Kasymov S.S. Laboratory Studies of Spatial Spectra of Radio Emission from Periodically Rough Water Surface. *Atmospheric and Oceanic Physics*, v.32, No.2, 183-185, 1996. (in Russian)
- Kravtsov Yu.A., Mirovskaya E.A., Popov A.E., Troitski I.A., Etkin V.S. Critical Effects in the Thermal Radiation of a Periodically Uneven Water Surface. *Atmospheric and Oceanic Physics*, v.14, No.7, 733-739, 1978. (in Russian)
- Liebe H.J. MPM - An atmospheric millimeter-wave propagation model // *Intern. J. of Infrared and Millimeter Waves*. 1989. V. 10. <sup>1</sup> 6. P. 631-650.
- Romeiser R., W. Alpers, V. Wismann, "An improved composite surface model for the radar backscattering cross section of the ocean surface 1. Theory of the model and optimization/validation by scatterometer data", *J. Geophys. Res.*, vol. 102, pp. 25237-25250, 1997.
- Sasaki Ya., Asanuma I., Muneyama K., Naito G., Suzuki T. The dependence of sea-surface microwave emission on wind speed, frequency, incidence angle, and polarization over frequency range from 1 to 40 GHz // *IEEE Trans. Geoscience and Remote Sens.* 1987. V. GE-25. <sup>1</sup> 11, P. 138-146.
- Swift C.T. Microwave radiometer measurements of the Cape Cod Canal // *Radio Science*, 1974, <sup>17</sup>, P. 641-653.
- Trokhimovski Yu.G., Etkin V.S. Laboratory and Field Studies of the Critical Phenomena under Thermal Microwave Emission of Waved Sea Surface. *Space Research Institute Tech. Memo.*, Pr-944, 23p., 1985. (in Russian)
- Trokhimovski Yu.G., Khapin Yu. B., Etkin V.S., Polarization and spectral characteristics of microwave emission of rough sea surface, *Tech. Rep.*, PR-821, Academy of Science USSR, Space Research Institute, Moscow, 36 pp., 1983, (in Russian).
- Trokhimovski Yu.G., Bolotnikova G.A., Etkin V.S., Grechko S.I., Kuzmin A.V. The dependence of s-band sea surface brightness temperature on wind vector at normal incidence // *IEEE Trans. Geosci. Remote Sensing*. 1995. V. 33, <sup>1</sup> 4, P. 1085-1088.
- Trokhimovski Yu. G., V. G. Irisov. The analysis of wind exponents retrieved from microwave radar and radiometric measurements, *IEEE Trans. Geosc. Remote Sens.*, v. 38, pp. 470-479, 2000.
- Trokhimovski Yu. G., V. G. Irisov, E. R. Westwater, L. S. Fedor, V. E. Leuski. Microwave polarimetric measurements of the sea surface brightness temperature from a blimp during Coastal Ocean Probing Experiment (COPE). *J. Geophys. Res.*, v. 105, pp. 6501-6516, 2000.

Trokhimovski Yu. G. Gravity-capillary wave curvature spectrum and mean square slope retrieved from microwave radiometric measurements (Coastal Ocean Probing Experiment). *J. Atm. Oceanic Techn.*, pp...., 2000.

Ulaby F.T., Moore R.K., Fung A.K. Microwave remote sensing: Active and Passive. Volume III. Artech House, Dedham, Mass., 1986, 2162 p.

Verevkin A.A. Il'in V.A., Irisov V.G., Kamenetskaya M.S., Lobova G.N., Maslennikov N.M., Trokhimovski Yu.G., Fatykhov K.Z., Etkin V.S. Laboratory Investigations of Critical Phenomena in the Thermal Radiation of Rough Water Surface by Means of Josephson Radiometer. Space Research Institute Tech. Memo., Pr-1413, 36p., 1988. (in Russian)

Wentz F.J. A model function for ocean microwave brightness temperature // *J. of Geophys. Res.* 1983. V. 88. <sup>1</sup> C3, P.1892-1907.

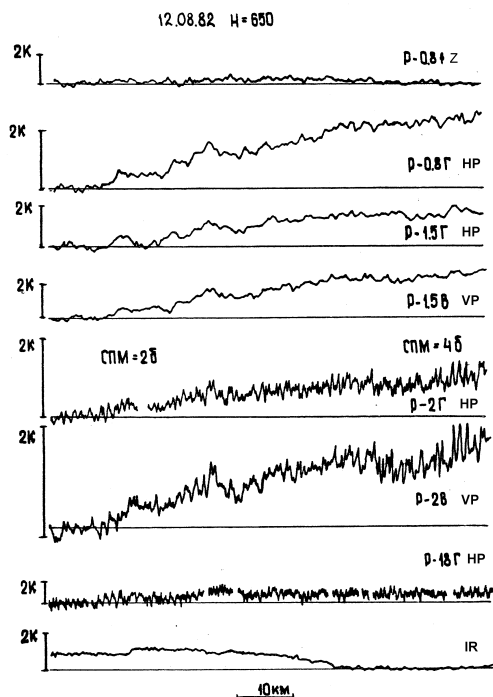


Fig. 1. Brightness temperate observed over sea surface with variable wind speed. Flight in wind direction. At the beginning wind speed is 4 m/c, at the end of record wind speed is 8-10 m/s. Using similar data we have determine “wind speed sensitivity” of the brightness temperature.

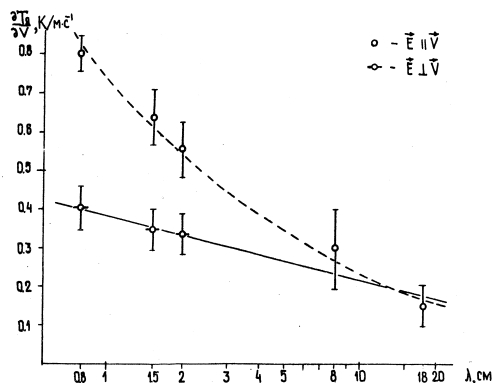


Fig. 2. "Wind speed sensitivity" of the brightness temperature from Russian experiments (aircraft AN-12). Nadir + data collected at view angles 10 and 20 degrees. Linear regression was used for wind from 4 to 10 m/s.

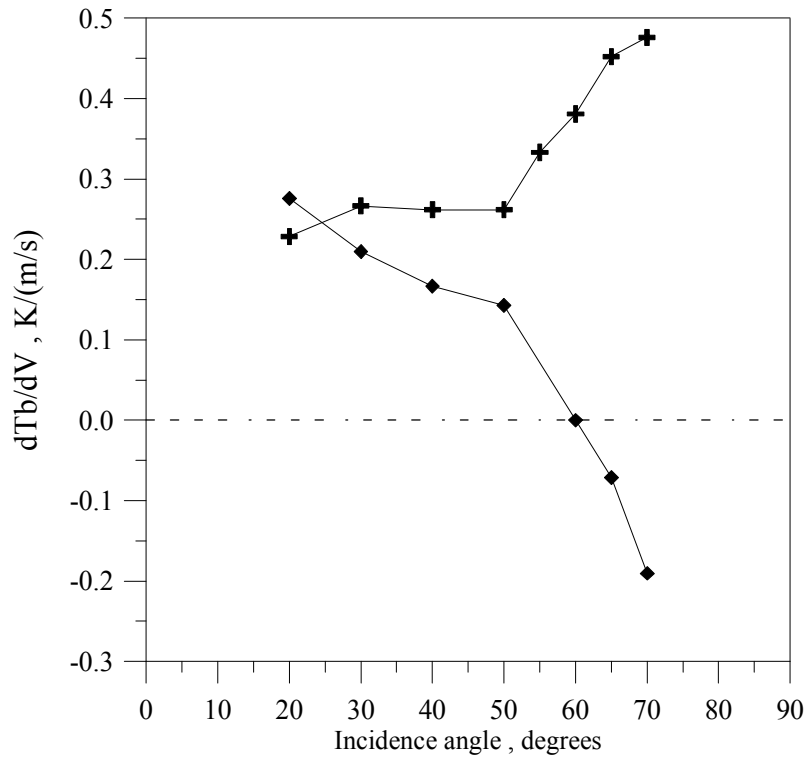


Fig. 3. L-band results by *Hollinger* [1971]. Frequency is 1.41 GHz. Mean wind sensitivity for wind range 0.5-13.5 m/s.

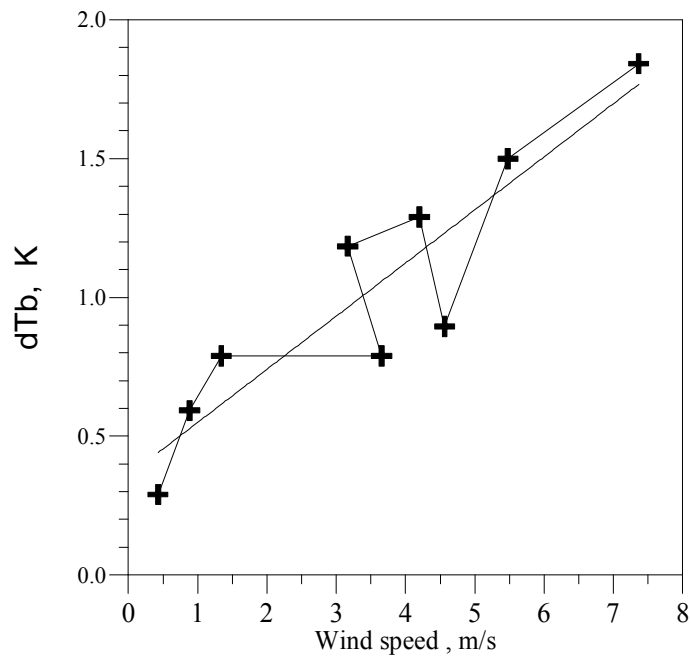
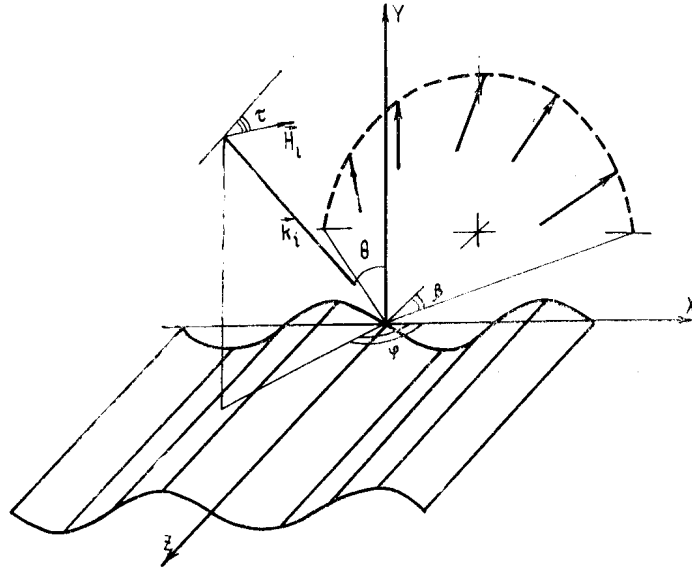


Fig. 4. Experimental results by *Blume et al.* [1977]. Frequency is 2.65 GHz ( $\lambda=12$  cm), nadir view.



$$K^2 \pm 2Kk \cos \varphi \sin \theta = k^2 \cos^2 \theta,$$

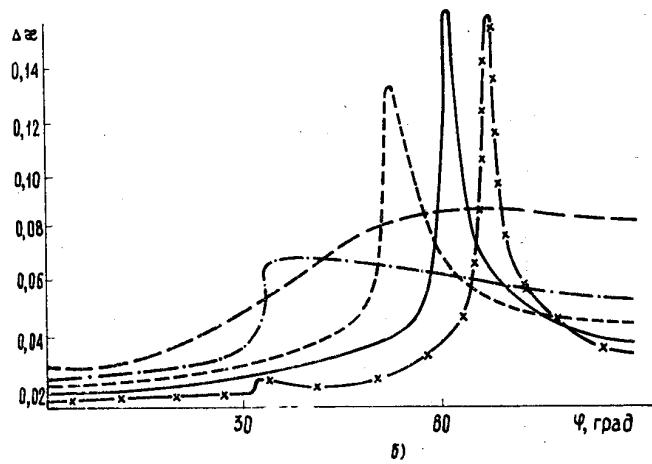


Fig. 5. Geometry, resonant condition and results of calculation in two-dimensional case. *Gershenson, Irisov, Trokhimovski, Etkin* [1987].

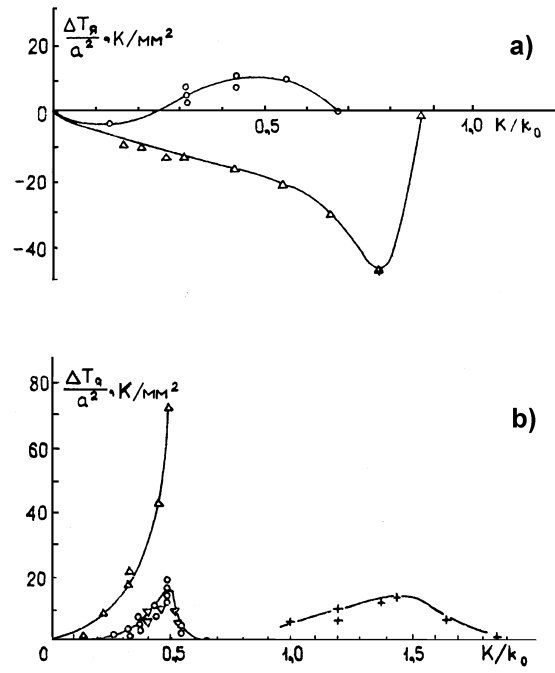


Fig. 6. Experimental test of the second order perturbation theory. *Etkin et al.*, [1978].

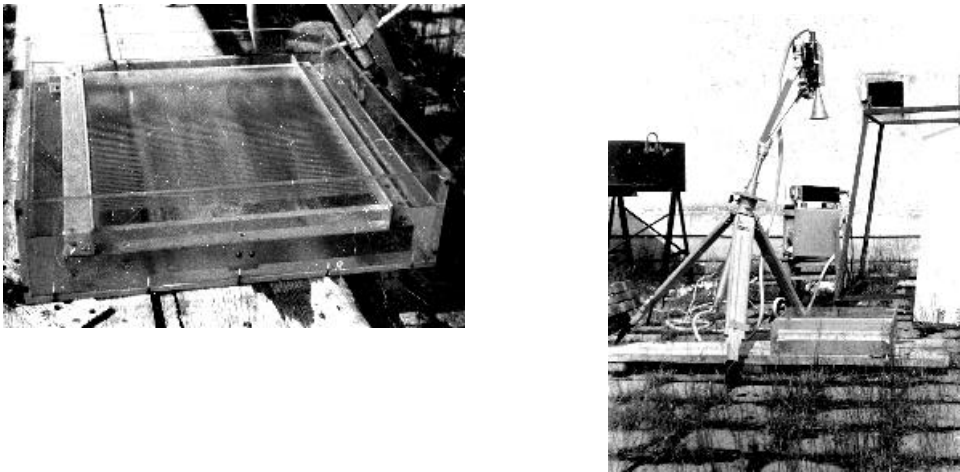


Fig. 7. Experimental facilities used for measurements.

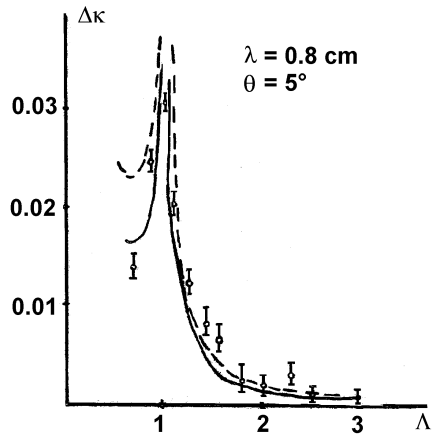


Fig. 8. Experimental study of resonance in brightness temperature. Trokhimovski, Etkin, [1985].

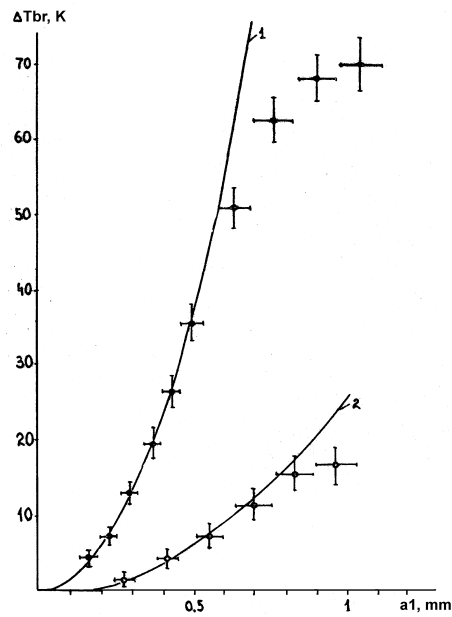


Fig. 9. Brightness temperature contrast at large ripple amplitudes. 1) *E* parallel *K*, 2) *E* perpendicular *K*. Trokhimovski, Etkin, [1985].

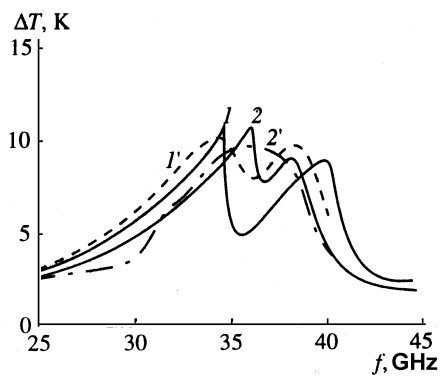


Fig. 10. Measurements using microwave interferometer. Il'in, Irisov, Kasymov, [1996].

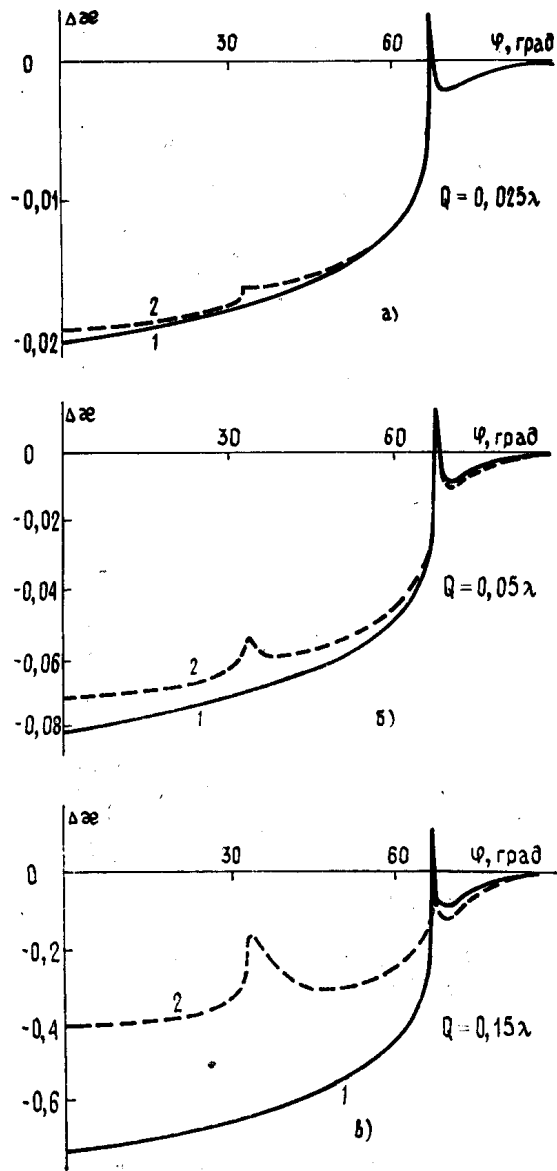


Fig. 11. 1) Small perturbation theory. 2) Numerical calculations.

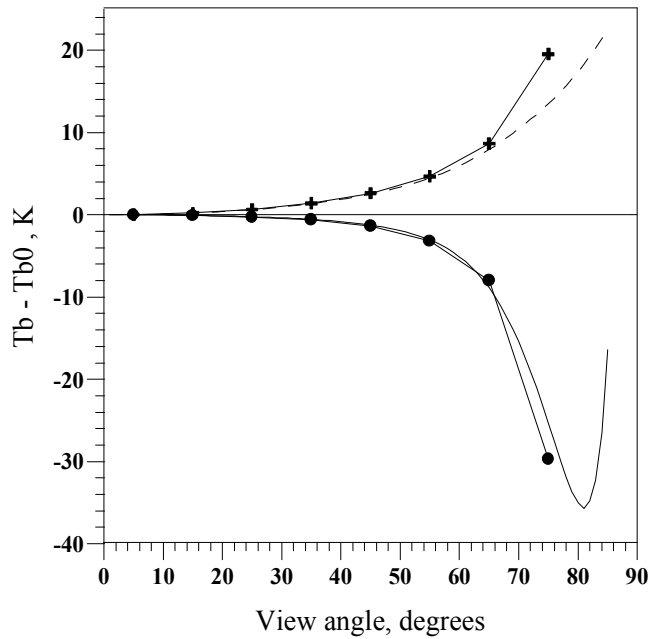


Fig. 12. Brightness temperature contrast at vertical (V) and horizontal (H) polarizations at wavelength 1.5 cm. Lines - Kirchgoff approach. Circles and crosses - small perturbation technique. Model power spectrum is used within the interval  $0.001 < K/k < 0.1$ . Height variance is equal to  $207 \text{ cm}^2$ , slope variances are  $\sigma_x^2 = 0.0238$  and  $\sigma_y^2 = 0.0237$ .

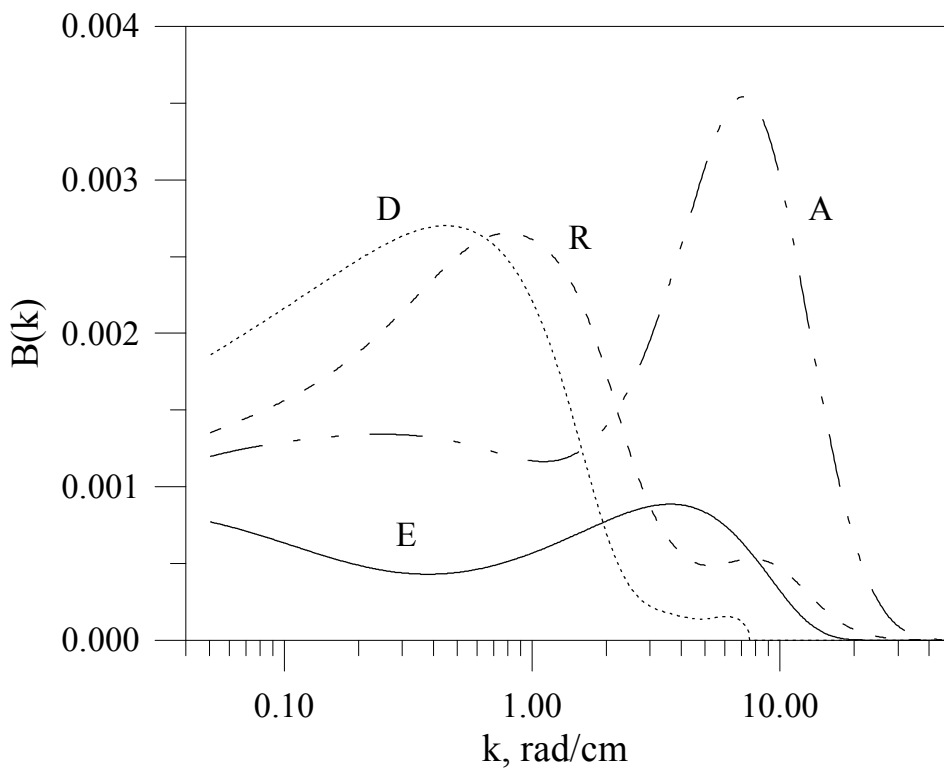


Fig. 13. Omnidirectional curvature spectrum of gravity capillary waves at wind speed 7.3 m/s ( $u_* = 24$  cm/s) as predicted by : *Donelan and Pierson* [1987] (D), *Apel* [1994] (A), *Romeiser et al.* [1997] (R), *Elfouhaily et al.* [1997] (E).

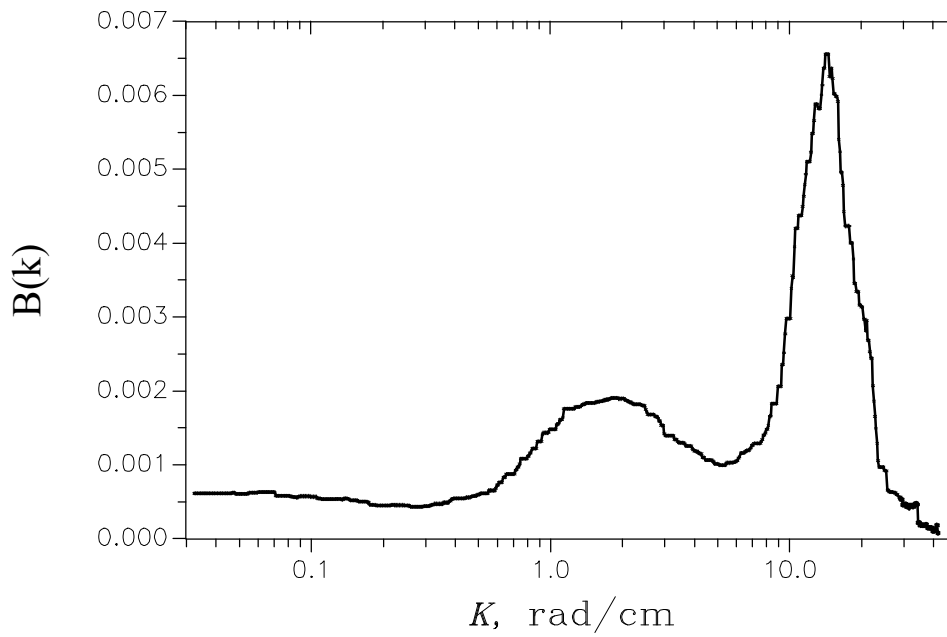


Fig. 14. “Best fit spectrum” retrieved by *Trokhimovski* [1997] using microwave radiometric data collected in different experiments.

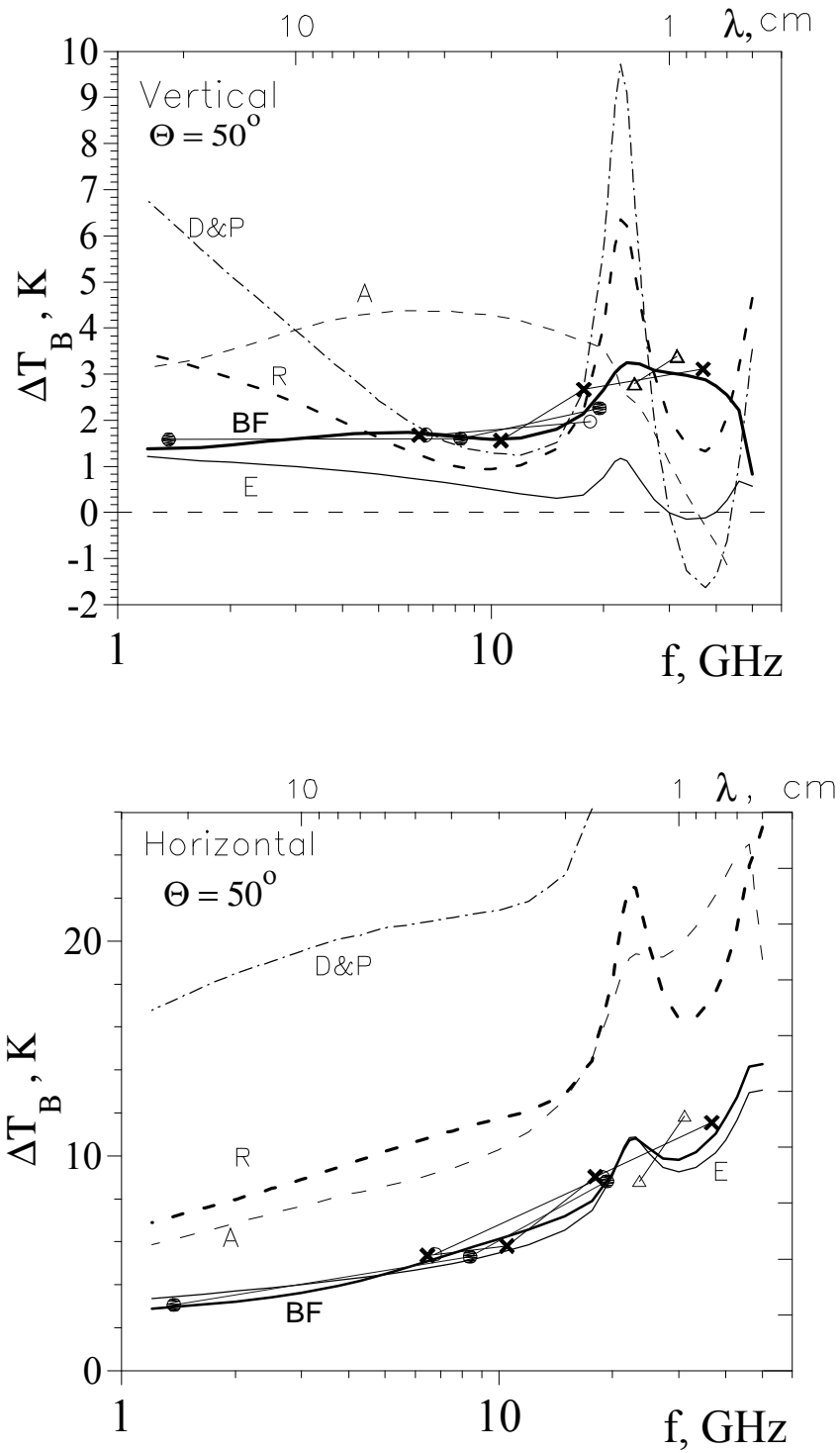


Fig. 15. The comparison between experimental data and calculations based on different spectrum models. Wind speed is taken 10 m/s, friction velocity is supposed to be 0.35 m/s. Experimental data summarized by *Sasaki et al.* [1987]. Solid circles - *Hollinger* [1970], crosses - *Wentz* [1983], open circles - *Sasaki et al.* [1987], open triangles - *Isozaki et al.* [1984].

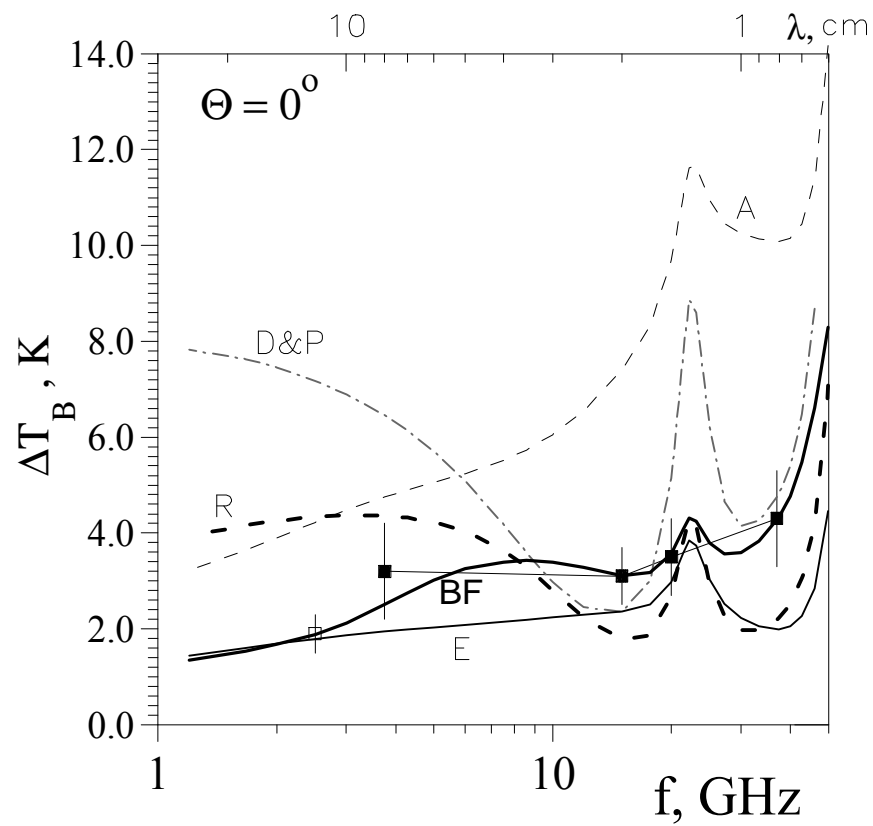


Fig. 16. The comparison between experimental data and calculations based on different spectrum models. Wind speed is taken 10 m/s, friction velocity is supposed to be 0.35 m/s. Nadir view. Solid squares are data by *Irisov, Trokhimovski, Etkin*, [1987]; open square is an extrapolation of the results by *Blume et al.* [1977].

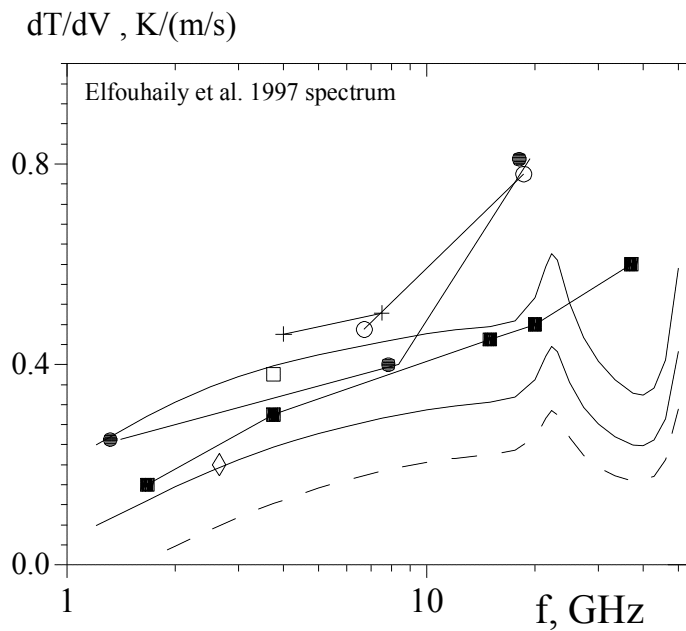
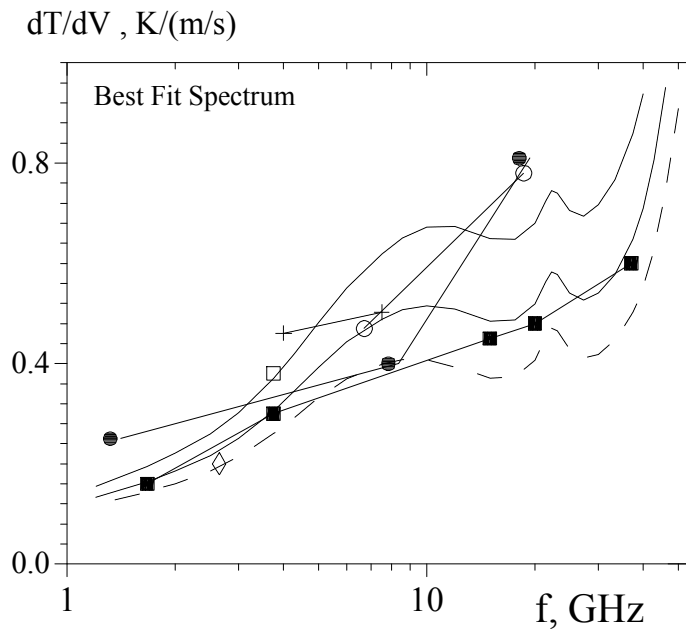
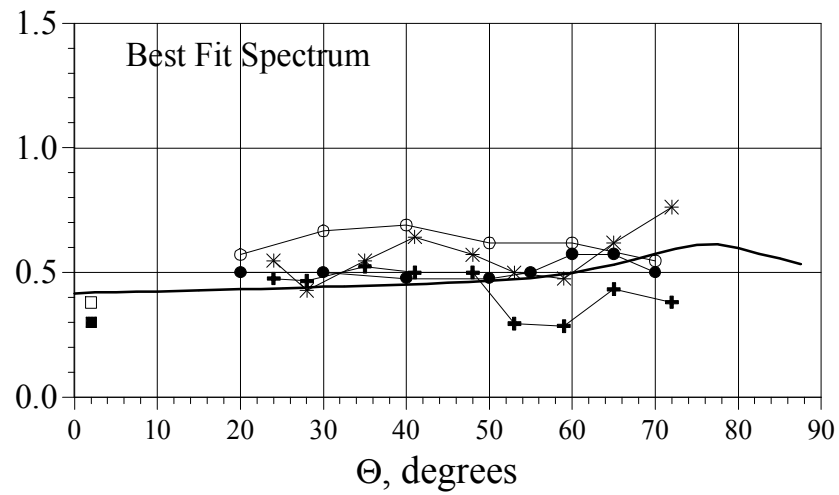


Fig. 17. Nadir wind speed sensitivity of brightness temperature on frequency. Modeling:  $V=6.1$  m/s - long dashed line,  $V=7.2$  m/s - solid line,  $V=8.7$  m/s - short dashed line. Experiment: solid circles - Hollinger, 1970,  $\theta=20^\circ$ ; crosses - Swift, 1974,  $\theta=25^\circ$ ; open rhomb - Blume et al., 1977,  $\theta=0^\circ$ ; solid squares - Trokhimovski et al., 1983,  $\theta=0^\circ$ ; open circles - Sasaki et al., 1987,  $\theta=20^\circ$ ; open square - Trokhimovski et al., 1995,  $\theta=0^\circ$ .

$dT_B/dV$ , K/(m/s)



$dT_B/dV$ , K/(m/s)

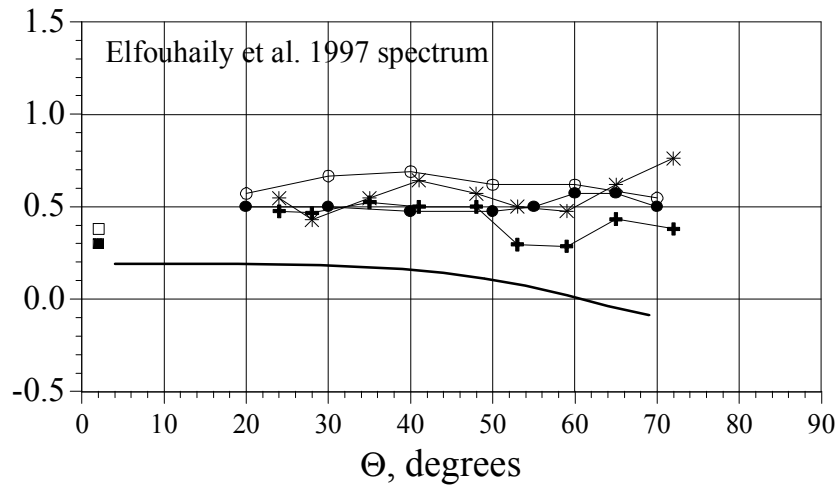


Fig. 18. Wind speed sensitivity. Horizontal polarization. Modeling is made for frequency  $f = 6$  GHz. Experiment: solid square - Trokhimovski et al., 1983,  $f = 3.8$  GHz; open square - Trokhimovski et al., 1995,  $f = 3.8$  GHz; crosses - Swift, 1974,  $f = 4.0$  GHz; open circles - Sasaki et al., 1987,  $f = 6.7$  GHz; snow stars - Swift, 1974,  $f = 7.5$  GHz; solid circles - Hollinger, 1970,  $f = 8.36$  GHz.

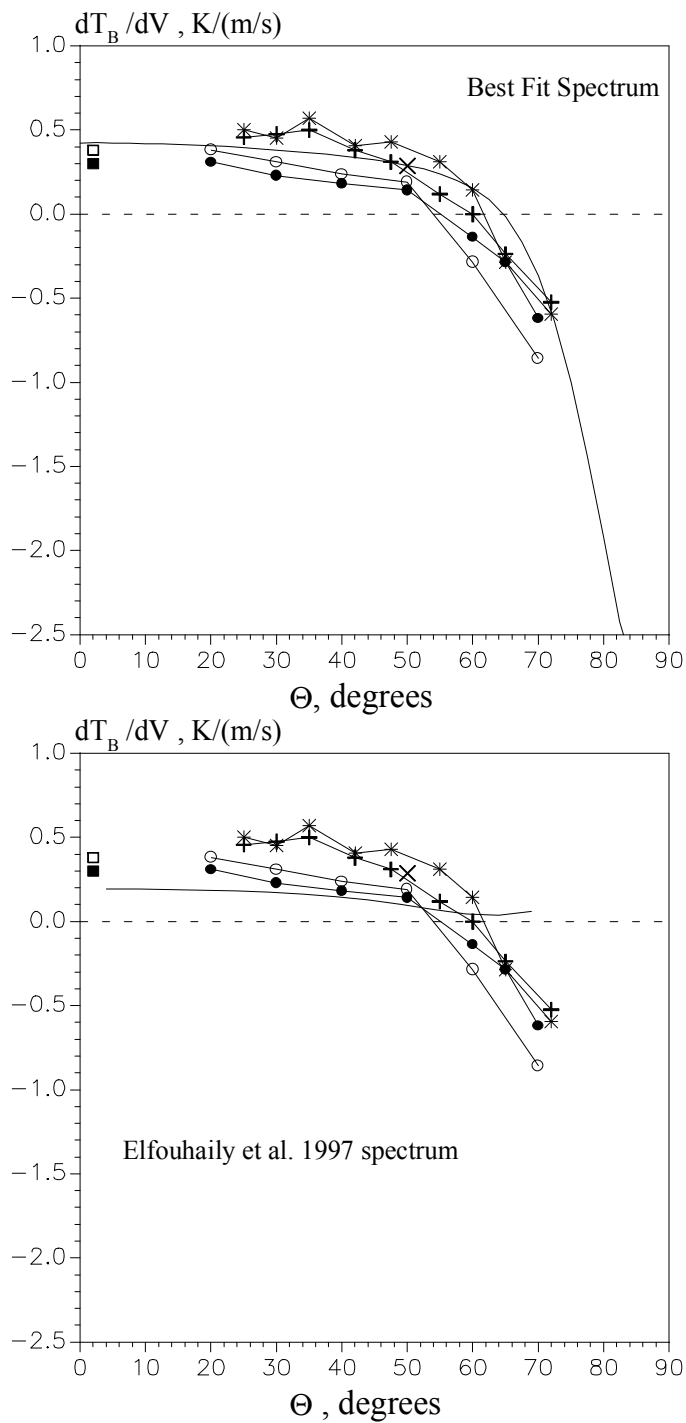


Fig. 19. Wind speed sensitivity. Vertical polarization. Modeling is made for frequency  $f = 6$  GHz. Experiment: solid square - Trokhimovski et al., 1983,  $f = 3.8$  GHz; open square - Trokhimovski et al., 1995,  $f = 3.8$  GHz; crosses - Swift, 1974,  $f = 4.0$  GHz; x - Wentz, 1983,  $f = 6.63$  GHz; open circles - Sasaki et al., 1987,  $f = 6.7$  GHz; snow stars - Swift, 1974,  $f = 7.5$  GHz; solid circles - Hollinger, 1970,  $f = 8.36$  GHz.

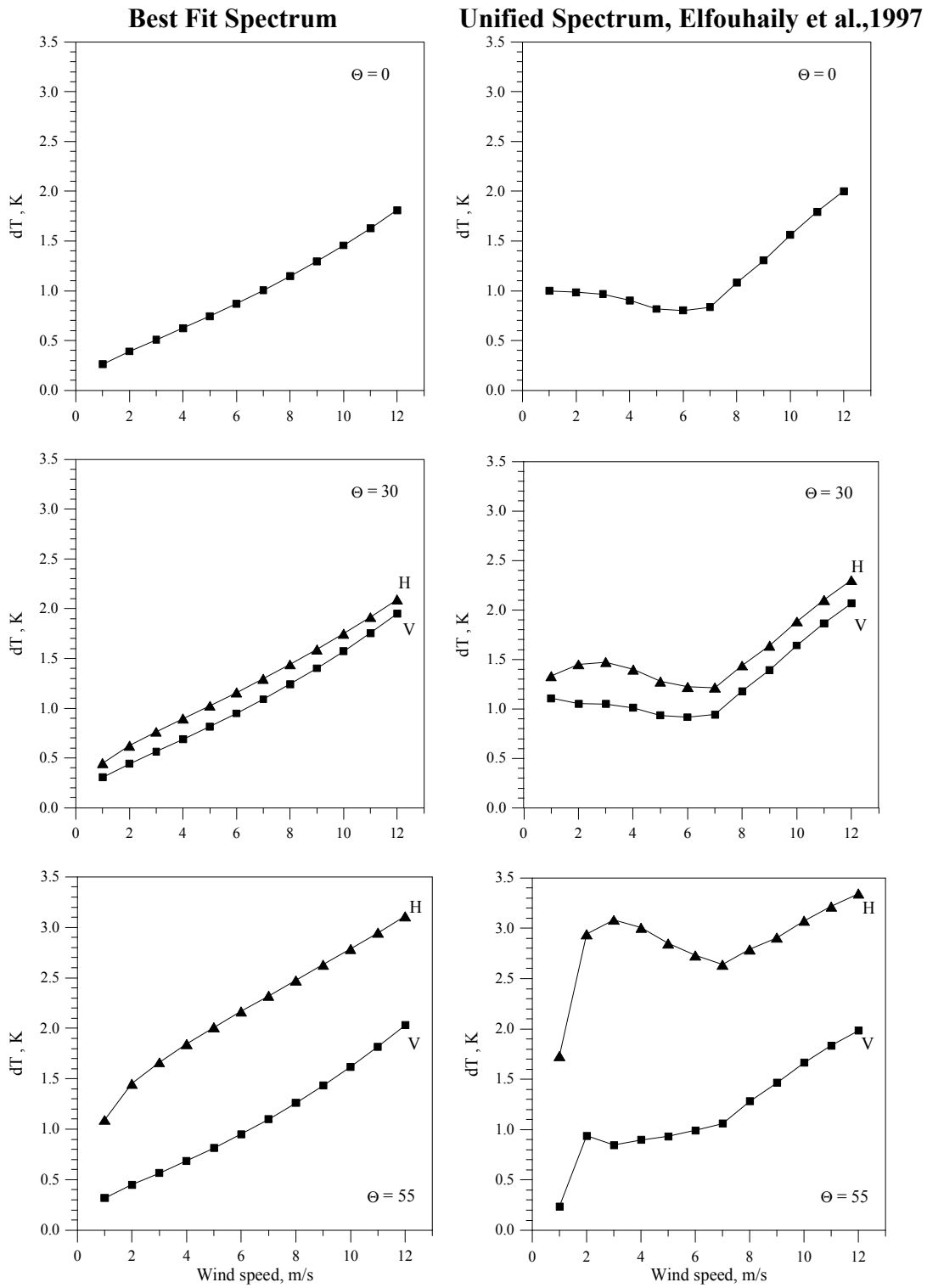


Fig. 20. L-band brightness temperature contrast as a wind speed function.

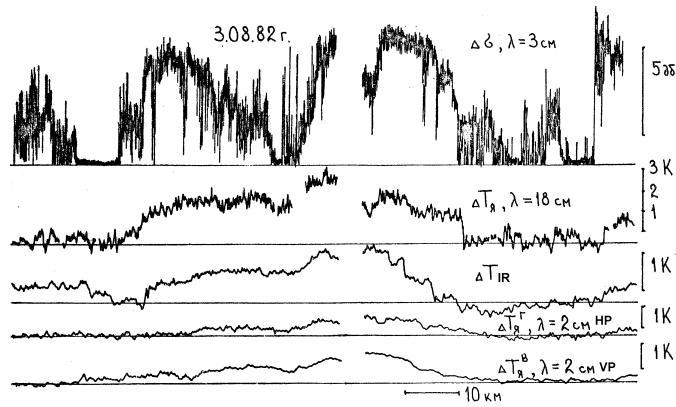


Fig. 20. Data collected at very low wind speed:  $V$  changes from 0 to 2-3 m/s, variable in space. Under such conditions L-band brightness temperature variations are extremely large. Their amplitude is larger than amplitude at wavelength 2, 1.5 and 0.8 cm.

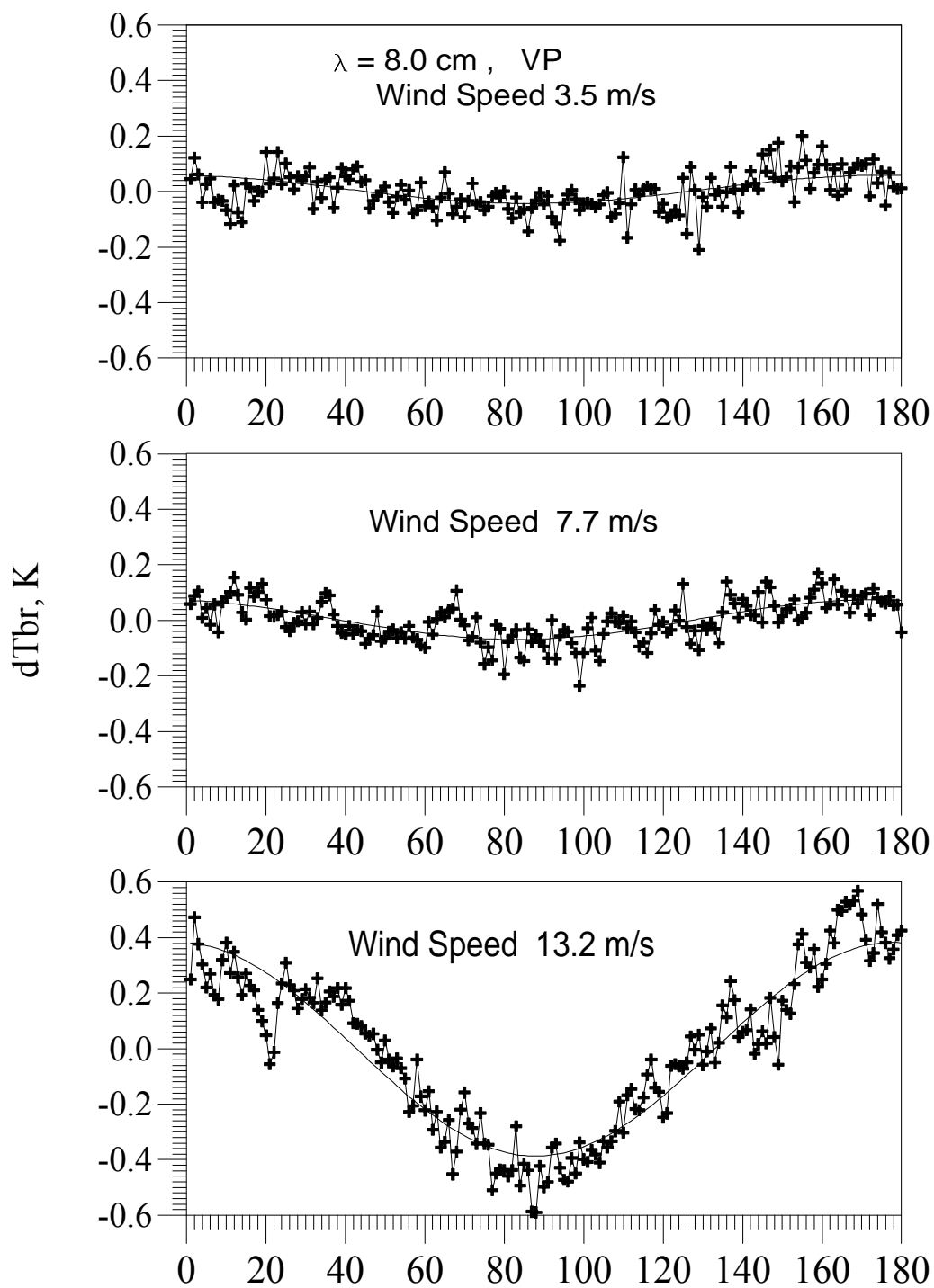


Fig. 21. C-band brightness temperature versus azimuthal angle calculated from wind direction. Nadir view.